ELSEVIER

Journal of Alloys and Compounds 330–332 (2002) 659–665

Journal of ALLOYS AND COMPOUNDS

www.elsevier.com/locate/jallcom

Hydrogen storage in carbon nanotubes and graphitic nanofibers

Vahan V. Simonyan, J. Karl Johnson*

Department of Chemical Engineering, University of Pittsburgh, Pittsburgh, PA 15261, USA

Abstract

We review experiments and computer simulations of adsorption of hydrogen on carbon nanotubes and on graphitic nanofibers. New results for adsorption of hydrogen on bundles of nanotubes intercalated with alkali metals are presented. The size and charge of the metal clusters is explicitly accounted for through a simple model. Charge transfer of electrons from the metal clusters to the nanotubes is also modeled. Results indicate that adsorption of hydrogen in metal-intercalated nanotube bundles is substantially enhanced compared with adsorption onto pure nanotubes. We compare simulations of adsorption in bundles with various lattice spacings to experimental results that claim swelling of nanotube bundles by adsorption of hydrogen. We find good agreement between the simulations and the experiments at higher pressures, indicating that hydrogen at 80 K probably does intercalate and swell nanotube bundles, thereby increasing the capacity of the sorbent.

Keywords: Fullerenes; Hydrogen storage material

1. Introduction

There has been a good deal of interest in the past several years in the possibility of storing hydrogen on single walled carbon nanotube (SWNTs) and graphite nanofibers. The hope is that these novel carbon materials have such highly uniform pore sizes, high surface areas, and attractive surface potentials that hydrogen can be adsorbed at high enough density to reach the US Department of Energy (DOE) targets for vehicular fuel cells. The DOE targets are reported to be about 6 wt.% for gravimetric and 60 kg/m^3 for volumetric densities [1]. The purpose of the paper is to review the experimental and theoretical work relating to adsorption of hydrogen on carbon nanotubes and graphitic nanofibers. We also present new simulation results for adsorption of hydrogen on pure nanotube bundles with various lattice spacings and on metal-doped SWNT bundles.

2. Hydrogen adsorption on commercial carbons

A wide variety of commercial and specialty carbons have been tested as possible sorbents for hydrogen storage. These include various activated carbons, carbon molecular sieves, carbon aerogels, and carbon fibers [1–5]. Experiments have consistently shown that carbon-based sorbents show very limited hydrogen uptake at room temperatures, typically less than 1 wt.% excess[1] adsorption. The general consensus is that commercial carbons are not effective sorbents for hydrogen storage at ambient temperatures. Molecular simulation of hydrogen physisorption on graphitic slit pore sorbents are in reasonably good agreement with many of the experiments on activated carbons [6–8]. Given that parallel graphitic slit pores are a very crude model for activated carbon, the agreement between experiment and simulation is a strong indication that hydrogen interacts with the sorbent through physisorption, that is, van der Waals forces rather than chemical forces, and that the solid–fluid potentials are reasonably accurate.

However, Orimo et al. [9] claim that nanostructured graphite can be made to hold up to 7.4 wt.% hydrogen if the graphite is prepared by extensive ball milling under a hydrogen atmosphere. Much of this hydrogen appears to be covalently bonded to the damaged carbon, but there is evidence that a large fraction of the hydrogen may be

*Corresponding author.

[1]Excess adsorption is defined as the total amount adsorbed minus the amount of fluid that would occupy the accessible volume at the density of the bulk fluid in equilibrium with the adsorbed fluid. At subcritical temperatures and low pressures the total and excess values are often very similar. At supercritical temperatures and high pressures the density of the bulk phase can be similar to the density of the adsorbed phase, resulting in a large difference between the values of the total and excess adsorption.

0925-8388/02/$ – see front matter
PII: S0925-8388(01)01664-4

intercalated between the graphite interlayers. The issue of releasing the hydrogen was not addressed.

3. Hydrogen adsorption on graphite nanofibers

Many of the recent results for hydrogen adsorption on SWNT and graphite nanofibers have been reviewed by Dresselhaus et al. [10]. Rodriguez et al. [11,12] claim to have observed incredibly high uptake of hydrogen onto graphitic nanofibers. Graphite nanofibers consist of catalytically produced graphene sheets that are oriented to form various fibrous structures. The orientation of the sheets in the fibers can be controlled by the choice of catalyst. The individual graphene sheets in these structures are thought to have very small cross-sectional areas, of the order of 50 nm^2. Hydrogen adsorption of up to 60 wt.% at 300 K and a pressure of about 100 atm on graphite nanofibers has been reported [11,12]. Experiments by different authors on graphite nanofibers have failed to confirm this very high adsorption [13,14]. However, Fan et al. have reported 10–13 wt.% adsorption [15]. Computer simulation studies of hydrogen adsorption on graphitic nanofibers [16] and graphitic slit pores [6,7,17] are unable to account for the phenomenal storage capacities reported by Rodriguez et al., or even for the more modest values claimed by Fan et al. The molecular simulations only account for physisorption of hydrogen, although Wang and Johnson [16] have demonstrated that even chemisorption is highly unlikely to account for the largest reported values of adsorption.

In a related experimental study, hydrogen adsorption on Pt-loaded carbon fibers has been studied as a way to test if hydrogen spillover could improve hydrogen uptake [18]. It was found that H/Pt ratios of up to 0.5 were achievable for Pt loadings of around 0.2 wt.%. The H/Pt ratio dropped by over an order of magnitude if the Pt weight percent was increased to around 2%. These results indicate that even hydrogen spillover onto carbon fibers is not capable of producing unusually large storage capacities.

Zhu et al. [19] studied the effect of surface treatment on the hydrogen storage capacities of materials they call carbon nanotubes. The materials they studied are not single walled carbon nanotubes, but appear to be closer to the graphite nanofibers studied by Rodriguez et al. [11,12]. Zhu et al. observe hydrogen adsorption ranging from 1 to 5 wt.% at room temperature and about 100 atm, depending on the pretreatment procedure. They observed that boiling the carbon material in 65% nitric acid for 72 h produced a sorbent that could store about 1 wt.% of hydrogen. The best performance resulted from treating the carbon material in NaOH. The size of the carbon structures appears to be of the order of several tens of nanometres. They claim that their treatment procedures produce micropores or etch grooves in the carbon materials, as well as introduce polar groups.

4. Hydrogen adsorption on carbon nanotubes

There have been a number of published experimental studies of hydrogen adsorption on SWNTs [20–26]. Dillon et al. were the first to publish reports of hydrogen adsorption by SWNTs [20,21]. Their initial work was carried out on samples containing only 0.1 to 0.2 wt.% nanotubes in a matrix of amorphous and graphitic carbon with residual Co catalyst. The hydrogen uptake by the SWNTs in the sample was estimated to be in the range of 5 to 10 wt.% for adsorption conditions of about 0.5 bar at 273 K, followed by a short exposure at 133 K prior to temperature programmed desorption (TPD). The estimated heat of adsorption from the TPD measurements was close to 20 kJ mol^{-1}. This value should be compared with 4 kJ mol^{-1} for H_2 on graphite [27] and simulation results of 6.3 kJ mol^{-1} [7] for hydrogen in SWNTs with about the same diameter as those observed in the experiment. More recent work by the same group indicates that uptake of about 7–8 wt.% is achievable on SWNT samples of high purity [28]. The TPD spectra show that about 2 wt.% hydrogen is released around room temperature, while the remainder of the hydrogen does not desorb until about 800 K. This seems to indicate that SWNT can adsorb about 2 wt.% through physisorption and about 6 wt.% more by some form of weak chemisorption from exposure to about 0.5 bar of hydrogen at room temperature [28]. Classical molecular simulations are not able to account for chemisorption, but should be able to account for the ~ 2 wt.% due to physisorption. We assume that the TPD method used by Dillon et al. measures the excess rather than the total adsorption. Theoretical studies of hydrogen adsorption on SWNTs have been carried out by molecular simulations [7,8,17,29–33] and adsorption density functional theory[2] [34]. None of the theoretical studies are able to account for 2 wt.% excess adsorption at 300 K and 0.5 bar. The excess adsorption predicted from theory at these conditions is almost two orders of magnitude lower than the experimental value. Our recent calculations indicate that the nanotube–H_2 interaction potential would need to be increased by a factor of four in order to achieve 2 wt.% adsorption at the experimental conditions [33].

Ye et al. reported hydrogen adsorption on purified SWNT samples at 80 K over a pressure range from 0.5 to 160 bar [22]. They observe very little adsorption at the lowest pressure. The amount adsorbed increases approximately linearly with pressure up to about 40 bar, at which point there is a change in slope as the adsorption increases more steeply with pressure (see Fig. 1). Ye et al. attribute

[2]Note that adsorption density functional theory should not be confused with electronic density functional theory. The former is a statistical mechanical theory for modeling adsorption of simple classical fluids in pores, while the latter is a method for solving the Schrödinger equation in terms of the electron density.

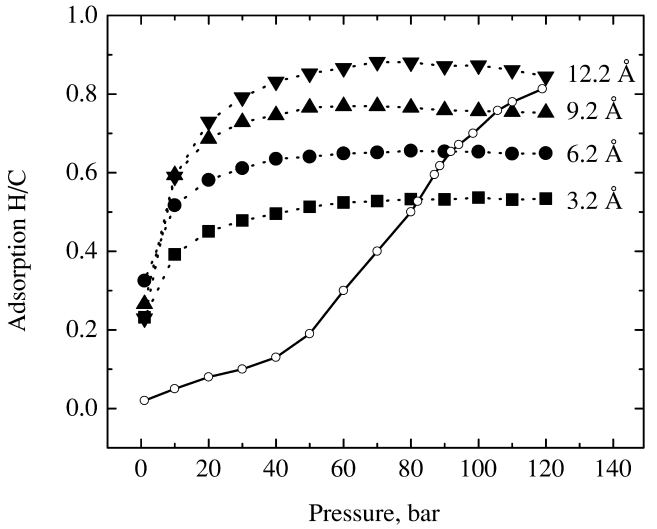

Fig. 1. Excess adsorption of hydrogen in a bundle of SWNT from simulations and experiment. The experimental results (solid line and open symbols) are from Ye et al. [22]. Simulations for bundles of nanotubes with different van der Waals gaps (distance between walls of neighboring tubes) are plotted as filled symbols. The lines are drawn as a guide to the eye.

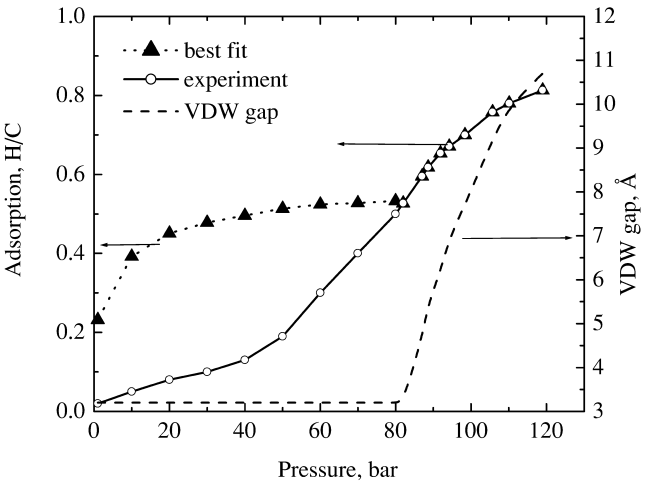

Fig. 2. The best fit of the simulation data to the experimental data from Ref. [22]. The van der Waals gap (VWD) for the tubes in the bundles are also plotted (dashed line).

the sudden change of slope to the swelling of the nanotube bundles by the hydrogen gas. We have performed molecular simulations of hydrogen adsorption on SWNT bundles at 80 K over a range of pressures. Details of the calculations are given elsewhere [29,30,33]. We have simulated a series of bundles with different van der Waals (VWD) gaps. The van der Waals gap is defined as the smallest distance between the walls of nearest neighbor nanotubes. The results of our simulations are plotted in Fig. 1 along with the experimental data from Ref. [22]. The excess adsorption from simulations at fixed lattice spacing behaves quite differently from the experimental isotherm. The simulations exhibit a maximum or a plateau in excess adsorption, which is a typical feature of adsorption of a supercritical fluid onto a rigid sorbent. In contrast, the experimental data show a monotonic increase in adsorption. The simulation data can be made to mimic the experimental data by choosing the VDW gap to be a function of pressure. This is shown in Fig. 2. Note that there is a qualitative difference between the shape of the experimental curve and the best curve that can be constructed from the simulations. At low pressures the simulations show substantially more hydrogen adsorbed than the experiments. At pressures greater than about 80 bar the simulation data can be mapped onto the experimental data by adjusting the VWD gap, which rises rapidly from close packing (3.2 Å) to about 11 Å. The disparity between simulation and experiment at low pressure may be due to kinetic effects or impurities in the sample. It may be that defect sites containing oxygenated groups [35,36] are blocking the entrance to some nanotube sites that somehow become available at higher pressures. We note that the measured surface area of the experimental sample (285 m^2/g) is considerably lower than the theoretical surface area of the close packed SWNT bundle ($\sim 1000\ m^2/g$). Scaling the simulation results by 0.3 to account for the difference in surface area would improve the agreement between simulation and experiment in the intermediate pressure range (between 20 and 50 bar), but the qualitative difference in the shape of the curves at low pressure would still persist. Notwithstanding the qualitative difference in the adsorption isotherms, we see that the magnitude of the uptake observed in the experimental isotherm can be reproduced from simulation by allowing the VDW gap between the nanotubes in the bundle to expand with increasing pressure. This gives at least indirect confirmation of the claim by Ye et al. that hydrogen is capable of swelling the nanotube ropes at high pressure [22].

Darkrim and Levesque [37] performed molecular simulation of hydrogen adsorption on arrays of carbon nanotubes of various diameters and with various VWD gaps at 77 K. They reported gravimetric densities in terms of total adsorption and compared these with experimental excess adsorption data of Ye et al. [22]. Given that the total adsorption is substantially higher than the excess, it is not surprising that they predicted larger adsorption than observed experimentally.

The electrochemical storage of hydrogen in materials containing SWNT has been studied [23]. A capacity of 0.39 wt.% hydrogen on a sample of gold pressed with a nanotube soot containing a small percentage of SWNTs. They speculate that high purity nanotube samples may be able to hold much more hydrogen [23].

Liu et al. [24] have reported hydrogen adsorption on samples containing ~ 50 wt.% nanotubes, with the remainder of the sample being composed of catalyst residue and

other carbons. They observe from 2.4 to 4.2 wt.% adsorption of hydrogen at 298 K and a pressure of about 100 bar. While Liu et al. do not explicitly state whether they are reporting total or excess adsorption, one would assume that the numbers are excess adsorption, since that is what is typically measured in an experiment. Computer simulations for an array of nanotubes at 298 K and 100 bar give between 0.3 and 1 wt.%, depending on the type of nanotube and the lattice spacing [29,33]. The total adsorption for the same systems lies in the range 0.5–2 wt.%.

Chen et al. reported that Li- or K-doped SWNTs can adsorb up to 20 wt.% hydrogen at temperatures around 600 K and a pressure of 1 atm [25]. However, a subsequent experiment on the same systems showed that the large weight gain was due to alkali hydroxide formation from a H_2 stream that was contaminated with water [26]. Experiments with ultrapure dry H_2 indicate that alkali-doped SWNTs are capable of adsorbing about 2 wt.% as measured by thermogravimetric analysis [26]. The hydrogen appears to be mainly chemisorbed.

It is worth noting that a recent theoretical study reported that (10,10) nanotubes could hold up to 14 wt.% hydrogen [38]. This study is unfortunately somewhat misleading. The authors use electronic density functional theory and a tight-binding formalism to study the geometry and chemical binding properties of atomic hydrogen inside and outside of an isolated SWNT. Tight binding studies can be very useful for chemically bonded species, but they do not give any information on long-range electron correlation, which is responsible for the physisorption phenomenon. Notably, the study indicates that chemisorption of atomic hydrogen on each carbon atom inside a nanotube is energetically unstable. The system relaxes to form molecular hydrogen inside the nanotube. However, their estimate of 14 wt.% is not realistic because the binding energies of the H_2 molecules are reduced by about 2 eV per molecule, indicating that the corresponding bulk pressure would have to be extraordinarily high, probably in the GPa range.

5. Adsorption on metal–nanotube compounds

Carbon nanotubes can be doped with electron donors and acceptors with resulting charge transfer to the SWNTs [25,26,39–43]. In a previous simulation we showed that charged SWNTs show an increased ability to store hydrogen [30]. We here present the first simulations of hydrogen adsorption on alkali metal intercalated SWNT bundles. Both the metal clusters and the charge transfer to the SWNTs are accounted for explicitly in the model.

5.1. Simulation details

The classical grand canonical Monte Carlo (GCMC) method was used to perform molecular simulations of hydrogen physisorption on SWNT samples. The average number of particles in the simulation box ranged from 100 to 10,000 hydrogen molecules. The systems were equilibrated for 5×10^5–10^6 simulation steps, followed by another 10^6 steps for data collection. Quantum effects were neglected although this could lead to an overestimation of the density by several percent at 77 K but a much smaller error at room temperature [7].

Imperfectly packed bundles were created from (8,8), (9,9), (10,10), (12,12) nanotubes. Nanotubes in the bundles were chosen randomly so the mean diameter was close to that for the (10,10) nanotube, which is the most abundant type of nanotube observed experimentally [44]. Bundles are not perfectly packed due to the non-uniform distribution of sizes. Despite the fact that experimentally observed nanotube ropes are usually bent over a distance of hundreds of nm, we considered only straight nanotubes since we expect that bending will have a small effect on adsorption.

Nanotube–lithium composites were designed by performing GCMC simulation of a Lennard–Jones solid on pure nanotube bundles with a VDW gap of 9.2 Å. This distance was chosen to accommodate octahedral and cubic clusters of lithium consisting of six to 10 atoms. The chemical potential during our simulations was chosen to provide about one Li atom per 10 carbons in order to model the experimentally observed nanotube–alkali composites [25,26,39–43]. The Lennard–Jones (LJ) parameters (see Table 1) for Li were chosen to satisfy the interatomic Li–Li distance of about 3.51 Å in cubic crystals and the theoretical binding energy of lithium binuclear clusters [45]. An example of a typical composite structure is shown in Fig. 3.

Charge transfer was modeled by uniformly charging the lithium clusters and nanotubes, locating the charges at the centers of atoms. The magnitude of the positive and negative charges were chosen to balance the lithium and carbon atoms (about $+1e/\mathrm{Li}$ and $-0.1e/\mathrm{C}$) so that the charge in the simulation unit cell was neutral.

5.2. Interaction potentials

All atomic (molecular) interactions were truncated at a distance of 20 Å. No long-range corrections were applied.

Table 1
Potential parameters for the interaction potentials

Parameter	Value	Parameter	Value
$P_{\parallel}$	0.57 Å^3	$\sigma_{Li_2-H_2}$	3.2 Å
$P_{\perp}$	1.995 Å^3	$\epsilon_{Li_2-H_2}$	136.8 K
P_H	0.81 Å^3	$\sigma_{Li_2-Li_2}$	3.51 Å
γ_H	0.314 Å^3	$\epsilon_{Li_2-Li_2}$	122.8 K
Θ_H	+0.63 esu		
E_H	2.337×10^5 K		
E_C	1.39254×10^5 K		

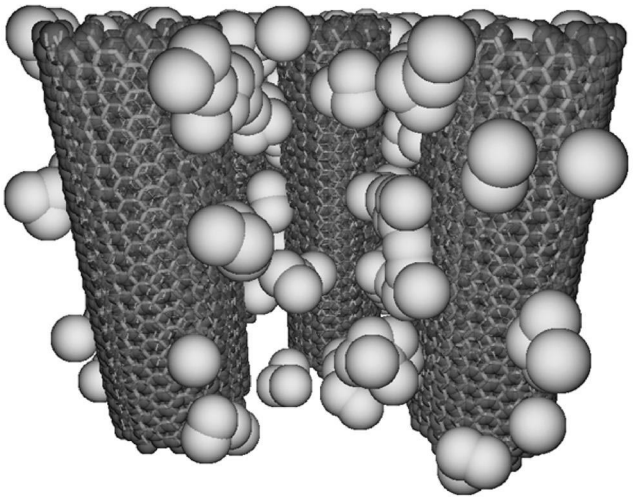

Fig. 3. Structure of the nanotube–alkali metal composite.

In a previous study we have shown that this cut-off is large enough to avoid substantially effecting the results [33].

The isotropic Silvera–Goldman [46] potential (SG) was used to describe the hydrogen–hydrogen interactions. The SG model treats each hydrogen molecule as a spherical center and includes the effects of three-body interactions through a pair-wise effective term. The semi-empirical SG potential has been found to be a good model for solid, liquid, and gaseous hydrogen [46–48].

The interaction of a hydrogen molecule with the adsorbent was calculated as a summation over all pair-wise interactions. The LJ potential was used to describe the interaction of the hydrogen molecules with the Li atoms. The parameters were fitted to agree with the theoretical estimate [45] of the H_2–Li_2 interaction energy (see Table 1). The Crowell–Brown anisotropic 6–12 potential [49] was used to model the dispersion and overlap interactions with nanotube

$$V_{\text{disp}} = \frac{E_{\text{H}}E_{\text{C}}P_{\text{H}}P_{\parallel}(1 + P_{\perp}/2P_{\parallel})}{r^{12}(E_{\text{H}} + E_{\text{C}})} + \frac{E_{\text{H}}E_{\text{C}}P_{\text{H}}\left[3(P_{\parallel} - P_{\perp})\cos^2(\alpha) + (P_{\parallel} + 5P_{\perp})\right]}{4r^{6}(E_{\text{H}} + E_{\text{C}})}, \quad (1)$$

where r is the distance between the center of mass of a hydrogen molecule and carbon atom in a nanotube, α is the angle between surface normal at the corresponding carbon atom position and the line connecting that atom with center of mass of a hydrogen molecule. Atomic polarizabilities and atomic characteristic energies are shown in Table 1.

The H_2-charge interactions were accounted for by including the two leading terms in the electrostatic potential,

$$V_{\text{polar}} = \frac{q^2P_{\text{H}}\left[1 + \frac{\gamma_{\text{H}}}{3P_{\text{H}}}(3\cos\theta^2 - 1)\right]}{8\pi\epsilon_0 r_i^4} + \frac{q\Theta_{\text{H}}(3\cos\theta^2 - 1)}{8\pi\epsilon_0 r^6}, \quad (2)$$

where r is the distance between center of mass of a hydrogen molecule and a point-charge location, θ is the angle between symmetry axis of the hydrogen molecule and r, q is the magnitude of the charge, Θ_{H} is the hydrogen quadrupole moment, and γ is the polarizability anisotropy of H_2. Parameter values are listed in Table 1. The first term of Eq. (2) describes the interaction of a point charge with the induced dipole of H_2. The second term describes the interaction of a charge with the permanent quadrupole of hydrogen.

5.3. Results

The results of hydrogen adsorption isotherms at 298 K on a metal-doped bundle and on the same bundle without the metal are shown in Fig. 4. The metal-free bundle does not include any electrostatic interactions. We observe from Fig. 4 that the adsorption at low pressures is very similar for the metal-doped and metal-free bundles on the scale of the figure. The actual adsorption is in fact larger for the metal-doped bundles even at the lowest pressure. Note that there is less free volume available for adsorption in the metal-doped bundles. Nevertheless, the enhanced adsorption potential due to the charge interactions more than compensates for the loss of free volume. At the highest pressure, the increase in adsorption in the metal-doped systems is close to 30%. This is a substantial increase, but

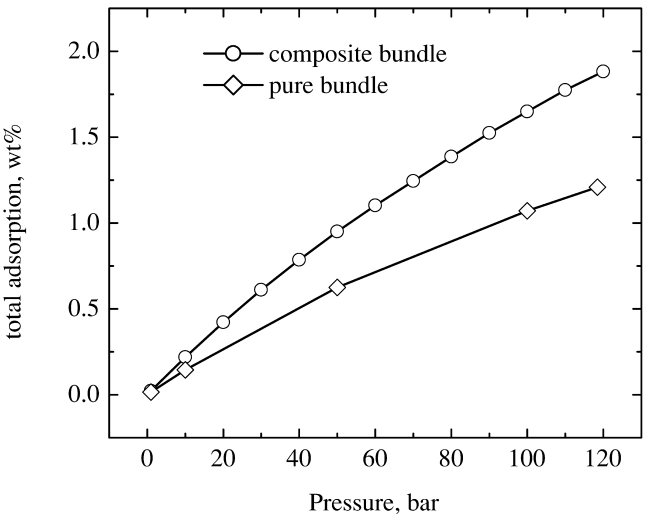

Fig. 4. Total hydrogen adsorption on an alkali metal-doped nanotube bundle (circles) and on the same bundle without the metal (diamonds). The temperature is 298 K.

not a dramatic one. These observations are consistent with previous simulations on charged nanotubes [30].

6. Conclusions

We have presented a review of experimental and theoretical work on hydrogen adsorption in graphite nanofibers and single walled carbon nanotubes. We have observed that there is a significant disparity between the experiments of Rodriguez et al. and the experiments and simulations from other groups. There does not appear to be any way to rationalize hydrogen uptake of the order of 50 wt.% within the framework of our current understanding of the physics of adsorption, whether by physisorption or chemisorption.

Experimental observations of excess hydrogen adsorption of several percent by weight at room temperature are larger than predicted from physisorption alone. Some sort of weak chemical binding of hydrogen onto the nanotubes may be responsible for the large uptake reported at room temperature.

Simulations of hydrogen adsorption on a bundle of nanotubes as a function of lattice spacing of the nanotubes indirectly confirms the observation that H_2 gas at 80 K can swell the nanotube bundle. An increase in excess adsorption as a function of lattice spacing was observed, and quantitative agreement with experiment was seen for pressures greater than 80 bar. At lower pressures there is a qualitative difference in the shape of the adsorption isotherms from theory and experiment.

Adsorption of hydrogen onto alkali-metal doped nanotubes was modeled using empirical potentials for the metal–nanotube and metal–hydrogen and electrostatic interactions. An increase in the total adsorption of almost 30% was achieved at 120 bar for the metal-doped nanotube bundle in comparison to the identical bundle without the metal and concomitant charge transfer. However, the total adsorption of hydrogen on metal-doped SWNT bundles is still a rather modest 2 wt.% which is significantly smaller than the DOE target.

Acknowledgements

Simulations were performed at the University of Pittsburgh Center for Molecular and Materials Simulations. This work was supported by grants from the Army Research Office and the National Science Foundation, CTS 9702239.

References

[1] S. Hynek, W. Fuller, J. Bentley, Int. J. Hydrogen Energy 22 (1997) 601.
[2] J.S. Noh, R.K. Agarwal, J.A. Schwarz, Int. J. Hydrogen Energy 12 (1987) 693.
[3] K.A.G. Amankwah, J.S. Noh, J.A. Schwarz, Int. J. Hydrogen Energy 14 (1987) 437.
[4] R. Chahine, T.K. Bose, Int. J. Hydrogen Energy 19 (1994) 161.
[5] P. Bénard, R. Chahine, in: J.C. Bolcich, T.N. Veziroglu (Eds.), Hydrogen Energy Progress XII, Vol. 2, International Association for Hydrogen Energy, Buenos Aries, 1998, pp. 1121–1130.
[6] Q. Wang, J.K. Johnson, Mol. Phys. 95 (1998) 299.
[7] Q. Wang, J.K. Johnson, J. Chem. Phys. 110 (1999) 577.
[8] F. Darkrim, D. Levesque, J. Chem. Phys. 109 (1998) 4981.
[9] S. Orimo, G. Majer, T. Fukunaga, A. Züttel, L. Schlapbach, H. Fujii, Appl. Phys. Lett. 75 (1999) 3093.
[10] M.S. Dresselhaus, K.A. Williams, P.C. Eklund, MRS Bull. 45 (1999), November.
[11] A. Chambers, C. Park, R.T.K. Baker, N.M. Rodriguez, J. Phys. Chem. B 102 (1998) 4253.
[12] C. Park, P.E. Anderson, A. Chambers, C.D. Tan, R. Hidalgo, N.M. Rodriguez, J. Phys. Chem. B 103 (1999) 10572.
[13] C.C. Ahn, Y. Ye, B.V. Ratnakumar, C. Witham, R.C. Bowman, B. Fultz, Appl. Phys. Lett. 73 (1998) 3378.
[14] R. Ströbel, L. Jörissen, T. Schliermann, V. Trapp, W. Schültz, K. Bohmhammel, G. Wolf, J. Garche, J. Power Source 84 (1999) 221.
[15] Y.-Y. Fan, B. Liao, M. Liu, Y.-L. Wei, M.-Q. Lu, H.-M. Cheng, Carbon 37 (1999) 1649.
[16] Q. Wang, J.K. Johnson, J. Phys. Chem. B 103 (1999) 277.
[17] M. Rzepka, P. Lamp, M.A. de la Casa-Lillo, J. Phys. Chem. B 102 (1998) 10894.
[18] J. Ozaki, W. Ohizumi, A. Oya, M.J. Illan-Gomez, M.C. Roman-Martinez, A. Linares-Solano, Carbon 38 (2000) 775.
[19] H.W. Zhu, A. Chen, Z.Q. Mao, C.L. Xu, X. Xiao, B.Q. Wei, J. Liang, D.H. Wu, J. Mater. Sci. Lett. 29 (2000) 1237.
[20] A.C. Dillon, T.A. Bekkedahl, K.M. Jones, M.J. Heben, in: K.M. Kadish, R.S. Ruoff (Eds.), Fullerenes, Vol. 3, 1996.
[21] A.C. Dillon, K. Jones, T.A. Bekkedahl, C.H. Kiang, D.S. Bethune, M.J. Heben, Nature 386 (1997) 377.
[22] Y. Ye, C.C. Ahn, C. Witham, B. Fultz, J. Kiu, A.G. Rinzler, D. Colbert, K.A. Smith, R.E. Smalley, Appl. Phys. Lett. 74 (1999) 2307.
[23] C. Nützenadel, A. Zütel, D. Chartouni, L. Schlapbach, Electrochem. Solid-State Lett. 2 (1999) 30.
[24] C. Liu, Y.Y. Fan, M. Liu, H.T. Chong, H.M. Cheng, M.S. Dresselhaus, Science 286 (1999) 1127.
[25] P. Chen, X.B. Wu, J. Lin, K.L. Tan, Science 285 (1999) 91.
[26] R. Yang, Carbon 38 (2000) 623.
[27] E.L. Pace, A.R. Siebert, J. Phys. Chem. 63 (1959) 1398.
[28] M.J. Heben, Private communications, 2000.
[29] Q.Y. Wang, J.K. Johnson, J. Phys. Chem. B 103 (1999) 4809.
[30] V.V. Simonyan, P. Diep, J.K. Johnson, J. Chem. Phys. 111 (1999) 9778.
[31] K.A. Williams, P.C. Eklund, Chem. Phys. Lett. 320 (2000) 352.
[32] G. Stan, M.J. Bojan, S. Curtarolo, S.M. Gatica, M.W. Cole, Phys. Rev. B 62 (2000) 2173.
[33] V.V. Simonyan, J.K. Johnson, in preparation.
[34] P. Gordon, P.B. Saeger, Ind. Eng. Chem. Res. 38 (1999) 4647.
[35] D.B. Mawhinney, V. Naumenko, A. Kuznetsova, J.J.T. Yates, J. Liu, R.E. Smalley, Chem. Phys. Lett. 324 (2000) 213.
[36] A. Kuznetsova, D.B. Mawhinney, V. Naumenko, J.T. Yates, J. Liu, R.E. Smalley, J. Am. Chem. Soc. 122 (2000) 2383.
[37] F. Darkrim, D. Levesque, J. Phys. Chem. B 104 (2000) 6773.
[38] S.M. Lee, Y.H. Lee, Appl. Phys. Lett. 76 (2000) 2877.
[39] A.M. Rao, P.C. Eklund, S. Bandow, A. Thess, R.E. Smalley, Nature 388 (1997) 257.
[40] R.S. Lee, H.J. Kim, J.E. Fischer, A. Thess, R.E. Smalley, Nature 388 (1997) 255.
[41] L. Grigorian, K.A. Williams, S. Fang, G.U. Sumanasekera, A.L. Loper, E.C. Dickey, S.J. Pennycook, P.C. Eklund, Phys. Rev. Lett. 80 (1998) 5560.

[42] L. Grigorian, G.U. Sumanasekera, A.L. Loper, S. Fang, J.L. Allen, P. Eklund, Phys. Rev. B 58 (1998) R4195.
[43] X. Fan, E.C. Dickey, P.C. Eklund, K.A. Williams, L. Grigorian, R. Buczko, S.T. Pantelides, S.J. Pennycook, Phys. Rev. Lett. 84 (2000) 4621.
[44] A. Thess, R. Lee, P. Nikolaey, H. Dai, P. Petit, J. Robert, C. Xu, Y. Lee, S. Kim, A. Rinzler, D. Colbert, G. Scuseria, D. Tomanek, J. Fischer, R. Smalley, Science 273 (1996) 483.
[45] D. Spelsberg, T. Lorenz, W. Meyer, J. Chem. Phys. 99 (1993) 7845.
[46] I.F. Silvera, V.V. Goldman, J. Chem. Phys. 69 (1978) 4209.
[47] Q. Wang, J.K. Johnson, Fluid Phase Equilibria 132 (1997) 93.
[48] Q. Wang, J.K. Johnson, Mol. Phys. 89 (1996) 1105.
[49] A.D. Crowell, J.S. Brown, Surf. Sci. 123 (1982) 296.